PCCP

Accepted Manuscript

ROYAL SOCIETY OF CHEMISTRY

www.rsc.org/pccp

Physical Chemistry Chemical Physics RSCPublishing

ARTICLE

Computer modeling of the complexes of Chlorin e6 with amphiphilic polymers

Cite this: DOI: 10.1039/x0xx00000x

Vladimir B. Tsvetkov[a,b], Anna B. Solov'eva[c], Nickolay S. Melik-Nubarov[d, *]

Received 00th January 2012,
Accepted 00th January 2012

DOI: 10.1039/x0xx00000x

www.rsc.org/

Recently it has been shown that Chlorin e6 (Ce6) complexes with Pluronics (hydrophilic ethylene and propylene oxide block copolymers) and poly(N-vinylpyrrolidone) (PVP) exhibit considerably higher phototoxicity towards tumor cells than free Ce6. The the present work was aimed to model Ce6 interactions with hydrophilic Pluronic F127 and PVP and find out the nature of intermolecular forces stabilizing these complexes. Modeling included 3 steps: (i) application of molecular dynamics to study polymer folding using AMBER 8 program, (ii) evaluation of partial charges in Ce6 molecule using different quantum mechanical, semi-empirical and topological approaches and (iii) docking analysis of Ce6 interaction with polymer coils using AUTODOCK 4.2. It was found that the folding in regular polymers does not occur stochastically, but goes through formation of "primary" helical structures, which further combined to form hairpin-like "secondary" structures. The latter in turn associated to form coil with minimal solvent accessible hydrophobic area. Ce6 ring resides flatwise on the surface of polymer coil in the interface between hydrophobic and hydrophilic regions. Calculations showed higher affinity of Ce6 to PVP in comparison to Pluronic and revealed marginal contribution of Coulomb forces in the stabilization of both complexes, which are mainly stabilized by van-der-Waals and hydrogen interactions.

Introduction

Photodynamic therapy is an approved modality for treatment of superficial tumors and festering wounds. It employs interaction of three components: light, photosensitizer and oxygen dissolved in biological tissues resulting in the generation of singlet oxygen, a powerful oxidizing agent capable of induction of necrotic and apoptotic processes in the target cells. [1,3] Application of polymeric carriers for photosensitizers is acknowledged as a powerful tool for enhancement of photodynamic therapy. Numerous publications report that binding of porphyrins to hydrophobic nanoparticles [3-5], nanogels [6-9] or amphiphilic polymers [10,11] can considerably increase photoinduced toxicity of porphyrins.

As for water-insoluble tetraphenylporphyrin [13], its derivatives [13-15] hydrophobic natural porphyrins verteporfin [16], protoporphyrin IX [10] and non-porphyrin photosensitizer hypericin [17], the nature of the complexes with amphiphilic copolymers and hydrophobic nanoparticles does not represent any riddle. In this case hydrophobic interactions solely determine stability of the polymer-porphyrin complexes. In contrast to this, the forces determining interactions of water-soluble porphyrins with amphiphilic and even hydrophilic polymers in water solution remain disputable and are the matter of investigation for the present report.

It has been found that binding of a hydrophilic photosensitizer Chlorin e6 (Ce6) to the hydrophilic polymer polyvinylpyrrolidone (PVP) strongly enhanced its contrast to tumor cells and its activity in photodynamic therapy. [18-31] Our own recent publication also revealed that Ce6 binding to hydrophilic Pluronics (F68, F87, F108 and F127) increased nearly by an order of magnitude its photosensitizing activity in cell cultures. [33] In contrast to this, hydrophobic members of Pluronic copolymers family did not influence Ce6 photodynamic activity. Nevertheless, a number of experimental data give evidence for the involvement of hydrophobic interactions in Ce6-PVP interactions. [18] So, it is obvious that the question about the nature of Ce6–polymer complexes is disputable.

Computer modelling of the complexes of low molecular weight drugs with synthetic macromolecules has been studied previously, strongly focusing on the complexes formed by highly ordered synthetic or semisynthetic polymers such as dendrimers [33,34] and cyclodextrins [35]. Molecular dynamics and docking studies of the complexes formed by water-insoluble antiandrogen agent bicalutamide with lactose, mannitol and hydroxypropylcellulose explained the nature of intermolecular forces favouring water solubility of these complexes. [36]

Study of interaction of low molecular weight drugs with synthetic linear polymers has been reported in only few papers up to now. Molecular dynamics (MD) was applied to model interactions of PEG-b-oligo(desaminotyrosyl-tyrosine octyl ester suberate)-b-PEG with highly lipophilic drugs paclitaxel, curcumin and vitamine D3, correlation between the drug hydrophobicity and its affinity to the polymer microspheres being observed. [37] MD simulations revealed non-binding interactions of PEG with paclitaxel and piroxicam, while strong attraction was observed between ethylene fragments of PEG and hematoporphyrin ring. [38] Noteworthy, the strength of these interactions was found to be dependent on the presence of salt in physiological concentration, indicating that coordination of metal cations by PEG may mediate its interaction with anionic porphyrins. Interaction of a number of polysaccharides, polyesters and PEG with a peptide immunosuppressant cyclosporine A was simulated using classical mechanical calculations, coupling strength being evaluated as energy of mixing. [39] Surprisingly, strong attraction of uncharged and highly hydrophobic cyclosporine A was observed not only to water insoluble L- and D- polylactides and polyglycolide, but to hydrophilic polymers cellulose and PEG and even to polyelectrolyte chitosan. Docking of N-acetyl-p-aminophenol on the surfaces of polybutyl- and polymethylmethacrylates successfully explained why crystallization of this substance on the surfaces of these closely related polymers results in quite different types of crystal lattice. [30]

So, application of molecular modelling assists in the understanding of molecular reasons for polymer-drug interactions. In the present paper we applied molecular dynamics simulations and docking analysis for the investigation of interaction of chlorin e6 with synthetic polymers. In this way, numerous approaches have been tested and quantitative agreement with the previously obtained experimental data has been achieved.

Methods

Chemical structure of Chlorin e6 (Ce6), Pluronic F127 and polyvinylpyrrolidone (PVP) are sketched in Fig. 1.

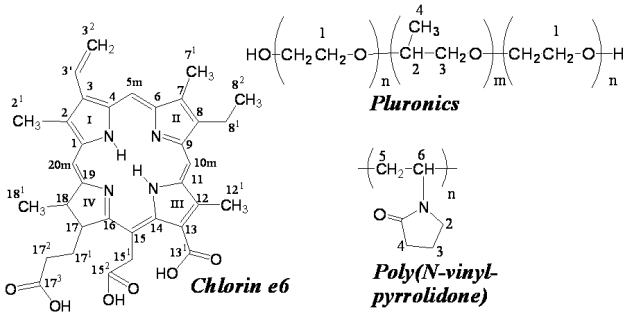

Fig. 1. Structure of Chlorin e6, Pluronic F127 and poly-N-vinylpyrroidone. Arab numerals denote numbers of carbon atoms in Ce6 and polymers and Roman numerals - numbers of pyrrole rings in Ce6 molecule.

The models of repeat units and chains for analyzed polymers were built in three dimensional (3D) coordinates by using SYBYL 8.0 molecular graphics software package (Tripos Inc., St. Louis, USA). The number of repeat units in the polymer chains was taken to be equal to 100 repeat units in the homopolymer PVP and 200 unites of ethylene oxide and 65 units of propylene oxide for Pluronic F127 block copolymer. Keeping in mind the huge model's size, modelling of the polymers folding into coils was carried out in implicit solvent and partial atomic charges on polymer atoms were determined by the Gasteiger-Hückel method [31]. The molecular dynamics (MD) simulations were performed by using a suite of programs AMBER 9 [33]. The use of implicit solvent was realized with application of Hawkins-Cramer-Truhlar (HCT) model [33] within GB/SA (Generalized Born/Solvent-Accessible Surface Area) formalism [34] in the presence of 0.1 M NaCl. GAFF (General AMBER Force Field) [35] was utilized for calculating interatomic interaction energy between the polymer atoms.

At the beginning of MD simulations, the models energy was minimized using 250 steps of the steepest descent followed by 250 steps of conjugate gradient. Then gradual heating to 300 K during 20 ps was performed. To avoid wild fluctuations for our system at this stage, weak harmonic restrains were used with a force constant of 5 kcal/ mol/Å^3 for all atoms of the complex except hydrogens. The SHAKE algorithm [36] was applied to constrain the bonds to hydrogen atoms that allowed using a 2 fs step. Dielectric constants of 1 (interior) and 80 (exterior) were employed in all GB-MD simulations. The production phase of MD simulations was carried out until the poymers folded into coils (about 5 ns). To control the temperature, Langevin thermostat was used with the collision frequency of 1 ps^{-1}.

To model Ce6 binding to the polymers, it was docked on the surfaces of their coils. The 3D model of Ce6 was created with application of above mentioned SYBYL 8.0. Taking into account that precision of docking results should depend on values of Ce6 partial atomic charges they were computed using different methods. In the beginning, molecular mechanics minimization of the Ce6 model was performed by using SYBYL 8.0 and Powell's method [37] belonged to the conjugate gradient family of minimization methods with the following settings: Gasteiger-Hückel charges, TRIPOS force field, [38] non-bonded cut-off distance equal to 8 Å, a distance-dependent dielectric function, the number of iterations equal to 500, the simplex method in an initial optimization, and 0.05 kcal·mol^{-1}·Å^{-1} energy gradient convergence criterion. The geometry of porphyrin ring and vinyl radical side group was fixed during minimization. After that, single-point energy quantum mechanics calculations were provided. Semi-empirical methods: PM3 [39], PM6 [40] and calculations by using density functional theory (DFT) with hybrid exchange-correlation functional B3LYP (Becke three-parameter (exchange), Lee, Yang and Parr (correlation) [41-43]) were employed. The 6-31G(d) and 6-311G(2d,2p) basis sets were used for calculations using DFT/B3LYP theory level. Thus obtained electron density distributions were further used for calculation of partial atomic charges in Ce6 molecule by application of several most widely employed theoretical approaches, namely: Mulliken's

population analysis scheme (MPA) [44], Natural population analysis (NPA) scheme [45,46], and CHELPG (Charges from Electrostatic Potentials using a Grid based method)) [47] based on the fitting of molecular electrostatic potentials (MEP).

All quantum mechanics simulations were carried out using the Gaussian 09 program [48]. Docking procedure of flexible ligand to the full surface of rigid targets was performed using AutoDock 4.2 [49]. Preparation of the target and ligand for docking procedure was carried out using AutoDockTools program (ADT Version 1.5.4). Partial atomic charges on the ligand's and target's atoms evaluated as described above were used unchanged in these calculations. The grid maps for docking studies were computed using the AutoGrid4. Grid center was placed on the target center, and 126×126×126 points with grid spacing of 0.375 were calculated. The hybrid genetic algorithm with local search also known as Lamarckian genetic algorithm (GA-LS) [50] was applied for searching most probable binding site. The parameters for GA-LS were used such as: a number of GA-LS runs - 50, a maximum number of energy evaluations, a maximum number of generations - 27,000, mutation and crossover rates were equal to 0.02 and 0.8, respectively. Pseudo-Solis & Wets parameters were used for local search and number of iterations was set to 300. Starting position and conformation of ligands were random. Step of rotation for torsion angle was equal to 50°. After docking, all structures generated were clustered up with RMS tolerance of 2Å from a lowest-energy structure. The vinyl radical side group was kept parallel to porphyrin ring plane during docking procedure.

Free energy of polymer-Ce6 interactions was estimated by a force field scoring functions according to:

$\Delta G_{binding} = \Delta G_{elec} + \Delta G_{vdW} + \Delta G_{hbond} + \Delta G_{desolv} + \Delta G_{tors}$

Coulombic contribution ΔG_{elec} was calculated using distance-dependent dielectric constant defined according to Mehler and Solmajer. Van der Walls interactions term ΔG_{vdW} was estimated with Lennard-Jones potential and atomic parameters [49] from AMBER Force Field (AD4_parameters.dat). For scoring of H-bond energy ΔG_{hbond} 10/12 potential was used with a maximal well depth of 5 kcal/mol at 1.9Å for hydrogen bonds with oxygen and nitrogen and was multiplied by the function estimating deviation scope from ideal H-bonding geometry. Desolvation energy term ΔG_{desolv} was estimated using the atomic fragmental volume and solvation parameters derived from the method of Stouten [50]. Conformational entropy contribution, ΔG_{tors} , is proportional to the quantity of rotatable dihedral angles in the ligand. Each term was multiplied by semi-empirical weighting constants obtained from regression analysis of binding data of large amount of protein-ligand complexes.

For more precise calculating of the solvent contribution to the binding energy, another scoring function ChemScore [51] of empirical type belonging to CSCORE module of Sybyl 8.0 was used. In these calculations complex configurations generated by AUTODOCK 4.2 were used. Since this program used models possessing polar hydrogens only, Ce6 models were prepared for CSCORE module calculations by addition of non-polar hydrogens. Then, every conformation was subjected to 100 iteration cycles of energy minimization as described above to eliminate unfavorable van-der-Waals interactions caused by the added hydrogens. The geometry of porphyrin ring and polymers remained unchanged during minimization.

Results and discussion

1. Simulation of the polymer coils using molecular dynamics

On the first step, 3D-models of coiled PVP and Pluronic were built. Although Pluronic F127 is aggregated in micelles, modelling was performed with a single Pluronic chain to simplify the computational procedures.

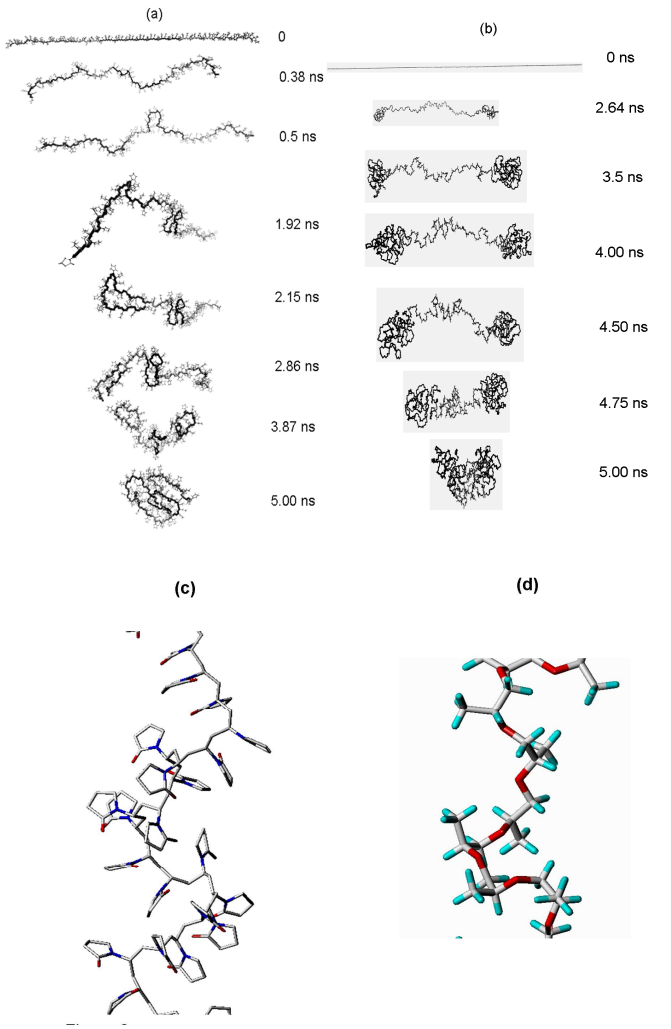

Fig. 2. Snapshots of MD simulations of polyvinylpyrrolidone (a,c) and Pluronic F127 (b,d) chains at 300 K corresponding to different points of stepwise folding of the chains in water environment (a,b). Panels (c) and (d) show enlarged images of helical structures formed in PVP (c) and PPO block of Pluronic (d)

MD simulations of PVP folding showed that it began from formation of small helical segments due to sterically constrained rotation around CH-CH_2 bond (Fig. 2a, panels corresponding to 0.38 and 0.5 ns, Fig. 2c). In about 2 ns these helices aggregated forming a hairpin with alkyl groups buried

inside and pyrrolidone carbonyls being exposed to the water environment.

Further evolution of the conformation resulted in the association of these hairpins and finally formation of a partially "ordered" coil in which less polar polyvinyl backbone had a tendency to be buried inside and water accessible surface was covered by hydrophilic pyrrolidone rings.

Similar behavior was recently reported for the folding of peptoid oligomer of N-substituted glycine, which spontaneously formed helical structures, although the kind of intrabackbone hydrogen bonding was precluded in these oligomers due to substitution of a single hydrogen atom in the amide bonds [53]. In this case, formation of helical structures was obviously caused by the constraint of rotation around amide bond in peptoid oligomers.

Peculiarities of Pluronic folding were determined by its tri-block architecture. Very flexible and unconstraint polyethylene oxide blocks underwent folding in the first few ns of the computational experiment without formation of any regular structures. In contrast to this, PPO block had a tendency to form helices resembling behavior of PVP. In this case formation of helical structures was obviously caused by constraint of rotation in -CH(CH_3)-CH_2-O torsion angle (Fig. 2d). Further evolution of the chain conformation resulted in association of the helices with formation of hairpins and, finally, folding in the compact coil partially screened from the surrounding water with more hydrophilic polyethylene oxide blocks.

MD simulations of Pluronic F127 folding were stopped at the moment when the dimensions of the second hydrophilic block matched those of the first one. The dimensions of the first hydrophilic and the central hydrophobic blocks reached plateau about 1.5 ns before the end of the computational experiment. Evolution of end-to-end distance and gyration radius of Pluronic chain illustrates that both hydrophilic blocks of Pluronic underwent folding during the first 2-3 ns of the simulation, while folding of PPO polypropylene oxide block began when PEO blocks has been already folded and occurred in an avalanche during further 1.5-2 ns (Fig. 3a).

Evaluation of the radius of gyration of PVP from the previously published value of its persistent length gives 16 Å [54] that is close to the value obtained by MD simulations (Fig. 3). This suggests that even in case of stereoregular polymers, MD simulations yield conformations with gyration radii close to those predicted by freely jointed chain model. At the same time, the conformation obtained from MD simulations of the stereoregular model chain corresponds to considerably oblate ellipsoid (Fig. 2a) in contrast to the spherical conformation adopted by freely-jointed chain. [55] Deviation of the conformation of stereoregular chain from spherical symmetry is obviously due to the hierarchy of the folding which proceeds via formation of helical and hairpin structures.

The tendency of isotactic synthetic polymers to form helical structures both in the solid and in solution has been documented previously. For example, this phenomenon is long known for isotactic polymethacrylic acid [56], which forms helical structures under acidic conditions. Similar phenomena were also described for other vinyl polymers [57]. In the experiments which stimulated the present work [22], atactic polymers were used. Therefore formation of helical structures in the systems seems to be improbable. Nevertheless, hierarchy of polymer coiling with formation of hydrophobic contacts and further statistically driven folding of the chain seems to be an important regularity revealed in the present work.

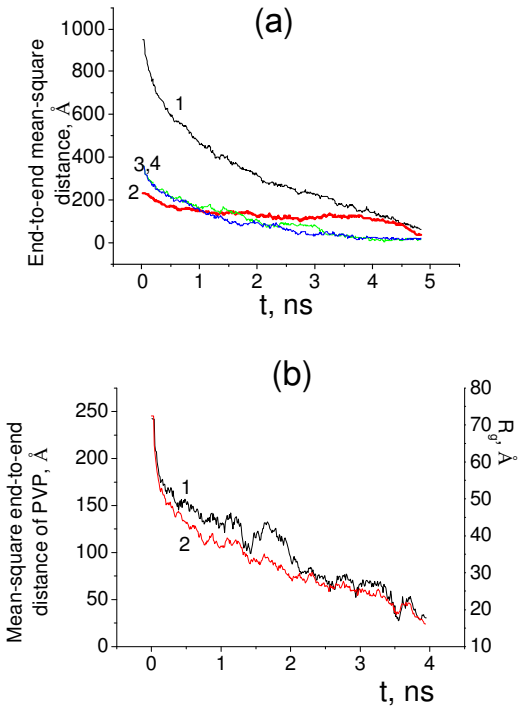

Fig. 3. Evolution of Pluronic F127 end-to-end distance (a) of the whole chain (1), its hydrophobic (2) and two hydrophilic (3, 4) blocks and (b) PVP end-to-end distance (1) and gyration radius (2) during the computational experiment at 300 K.

Calculation of partial charges in Ce6.

Investigation of Ce6 interaction with the pre-formed coils of PVP and Pluronic F127 requires building of Ce6 model, and in particular, partial charges of atoms in Ce6 molecule should be evaluated. Unfortunately, we were unable to find in the literature reliable and generally accepted methods allowing calculation of local charges in porphyrins. Therefore, in search of the scheme for evaluation of partial atomic charges in Ce6, we tried three approaches usually being applied for this purpose: topological, semi-empirical and DFT-based. So, total 9 schemes of partial charges evaluation were used and their results were compared with experimental data concerning NMR chemical shifts (Table 1). This comparison is based on the classical work of Gasteiger and Marsili [58] and more recent papers [59,60] where a considerable correlation between partial charges on carbon and proton atoms and their chemical shifts in ^{13}C- and ^{1}H-NMR has been established. The applied approach allows selecting schemes of partial charges evaluation appropriate to the particular class of compounds.

Calculation of electronic density distribution DFT/B3LYP density functional was applied with 2 Pople basis sets, 6-311G(2d,2p) and 6-31G(d), one of which (6-31G(d)) is routinely applied for the calculation of synthetic organic molecules, and the other (6-311G(2d,2p)) has been successfully applied for the calculation of electronic spectra of Ce6 [61]. Thus obtained wave functions were used to assign a specific part of the molecular electronic density to each atom using CHELPG analysis based on the grid based calculation of charges from electrostatic potential [47], Mulliken population analysis (MPA) based on the linear combination of atomic orbitals [44] and natural population analysis (NPA) based on the construction of a set of "natural atomic orbitals" [45, 46]. Within semi-empirical approach we applied PM3 and PM6 methods based on Neglect of Diatomic Differential Overlap [39, 40] that were selected as ensuring most precision. Within topological approach, Gasteiger-Hückel method was selected due to its good applicability for highly conjugated systems. Influence of polar water environment on partial charge distribution in Ce6 molecule was estimated using a Polarized Continuum Model (PCM) using the C-PCM polarizable conductor calculation model. [62, 63]

All methods of partial charges evaluation showed that carboxylic carbons (13^1, 15^3 and 17^3) have large positive charge, while those in meso-positions (5m, 10m, 15, 20m) and in the vinyl side group (3^1 and 3^3) are negatively charged. Carbons of NH-containing I and III pyrrole rings (atoms 1, 4, 11, 13) were slightly charged, while similar atoms in the II and IV pyrrole rings displayed pronounced positive charges due to negative charges on pyrrole nitrogens (Fig. 4 and the Table of partial charges in ESI).

Despite the fact that all methods of partial charges evaluation gave qualitatively similar results for strongly charged atoms (Fig. 4), the variety of partial charges of hydrogens and slightly charged carbons evaluated by different methods was striking. For example, partial charge of carbon atom in the position 8^1 was about -0.22 according to PM6 and +0.32 according to CHELPG grid-based method for DFT/B3LYP/6-311G(2d,2p) level of theory (Table 1).Such variation can influence the results of modelling; therefore we made an attempt to select most reliable methods comparing the results with experimentally available chemical shifts of carbons and hydrogens taken from ^{13}C-NMR and ^{1}H-NMR spectra.

Previously, it has been noted that such analysis is befogged by anisotropic effects by π-electron system of the porphyrin ring. [58Error! Bookmark not defined.] As far as these effects appear in the magnetic field, they cannot be completely considered by partial charges evaluation methods and worsens correlations. However even in complicated cases positive correlation between partial charges and chemical shifts is commonly observed. [59Error! Bookmark not defined., 60]

Analysis of linear correlations between the charges of hydrogen atoms evaluated by different approaches with their chemical shifts in ^{1}H-NMR in water [22] and pyridine-d5 [64] solutions (Fig. 5a) and ^{13}C-NMR in C^3HCl_3 solution allowed considering how the methods of partial charge evaluation correspond to the experimental values of chemical shifts. Correlation coefficients of linear dependencies between chemical shifts δ and local charges Δq varied from -0.299 to +0.92 for protons and in the range from +0.5 to +0.9 for carbon atoms (Fig. 5).

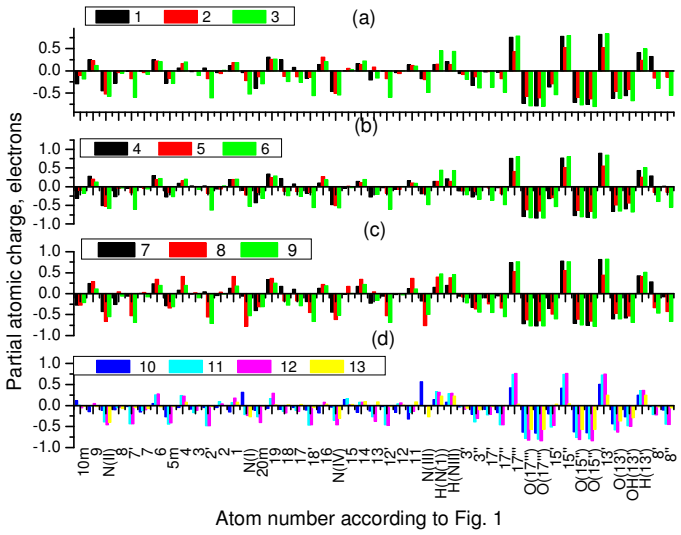

Fig. 4. Diagram of partial atomic charges of selected atoms in Ce6 molecule evaluated at DFT/B3LYP level of theory in combination with 6-311G(2d,2p) basis set and CHELPG, MPA and NPA methods of partial charges calculation in the presence of water (a); (4), (5), (6) – for similar scheme but in the presence of water(b); (7), (8), (9) – with the same method of partial charges calculation, but for 6-31G(d) basis set and in the absence of water (c); (10) and (11) - partial charges obtained by PM3 and PM6 semi-empirical methods in the absence of water and (12) by PM6 in the presence of water; (13) – partial charges calculated by Gasteiger-Hückel - topological approach (d). Values of charges of all atoms in Ce6 molecule evaluated by different approaches are available in supporting material.

Thus, charges of carbon atoms obtained from the schemes of Natural and Mulliken population analysis at DFT/B3LYP/6-31G(d) level of theory more or less regularly increased with the elevation of their chemical shifts obtained from ^{13}C-NMR data (squares in Fig. 5a for NPA with 6-31G(d) basis set), correlation coefficients being varied in the range 0.75–0.85 (Table 1).

In contrast to this, MPA charges on hydrogen atoms did not correlate with ^{1}H-NMR chemical shifts (R~-0.02-0.4) (Table 1). At the same time, Natural population analysis applied with both basis sets gave partial charges which exhibited satisfactory correlation with ^{1}H-NMR data (R~0.73-0.78) with exception of the atoms located in meso-positions and vinyl radical, whose signals are in the extremely weak field (6-10 ppm) since their nuclei experienced strong influence of the porphyrin ring current in the magnetic field. So, it may be concluded that NPA method applied at DFT/B3LYP level gives realistic charge distribution in Ce6 molecule independently, if 6-31G(d) or 6-311G(2p,2d) basis sets were used.

Another approach for partial charges calculation, grid-based CHELPG applied at DFT/B3LYP level of theory with both 6-31G(d) and 6-311G(2d,2p) data sets gave partial charges which exhibited satisfactory correlation with proton chemical shifts obtained in pyridine-d5 [64] and D_2O [22] both (asterisks in Fig. 5b), but exhibited poor correlation with carbon chemical shifts (squared in Fig. 5b). Correlation coefficients of the corresponding dependencies were about 0.5 for carbons and about 0.8 for hydrogen atoms (Table 1), indicating that this method gives more realistic estimates both for hydrogen and carbon atoms.

TABLE 1. Methods of evaluation of partial atomic charges in Ce6 molecule and parameters of linear correlations between the resulting charges of hydrogen and carbon atoms with ^{1}H-NMR[22] and ^{13}C-NMR **Error! Bookmark not defined.** chemical shifts.

Level of theory	Method of calculation of partial atomic charges	Correlation coefficient with ^{1}H-NMR chemical shifts	Correlation coefficient with ^{13}C-NMR chemical shifts
Quantum mechanical DFT-based approaches			
DFT/B3LYP/ 6-311G(2d,2p)	CLELPG without water	0.794	0.49
	MPA without water[a]	0.236	0.780
	NPA without water[a]	0.735	0.87
	CHELPG with water	0.811	0.5
	MPA with water[a]	-0.02	0.77
	NPA with water[a]	0.694	0.88
DFT/B3LYP/ 6-31G(d)	CLELPG without water	0.778	0.54
	MPA without water[a]	0.41	0.84
	NPA without water[a]	0.73	0.89
Quantum mechanical semi-empirical approaches			
PM3 without water		0.814	0.680
PM6 without water		0.294	0.830
PM6 with water			
Topological apprtoach			
Gasteiger-Hückel w/o water		0.920	0.470

[a] Chemical shifts of hydrogen atoms in meso- and vinyl positions in Ce6 were omitted from the correlations by virtue of significant influence of porphyrin ring current induced by external magnetic field.

Partial charges estimated with semi-empirical PM3 and PM6 methods exhibited moderate scattering for carbon and hydrogen atoms both. In this case, considerable divergence was observed for methyl carbons that hardly can be explained by anisotropy effects. Obviously, the estimate of partial charges in Ce6 given by these methods is very rough and can be used only for preliminary use. Correlation coefficients of linear dependencies between the charges of carbon and hydrogen atoms were 0.68 and 0.81 for ^{13}C-NMR and ^{1}H-NMR data correspondingly. PM6 charges displayed better correlation with ^{13}C-NMR (R~0.83), but worse with ^{1}H-NMR chemical shifts (R~0.55 and 0.3 with and without water correspondingly, Table 1).

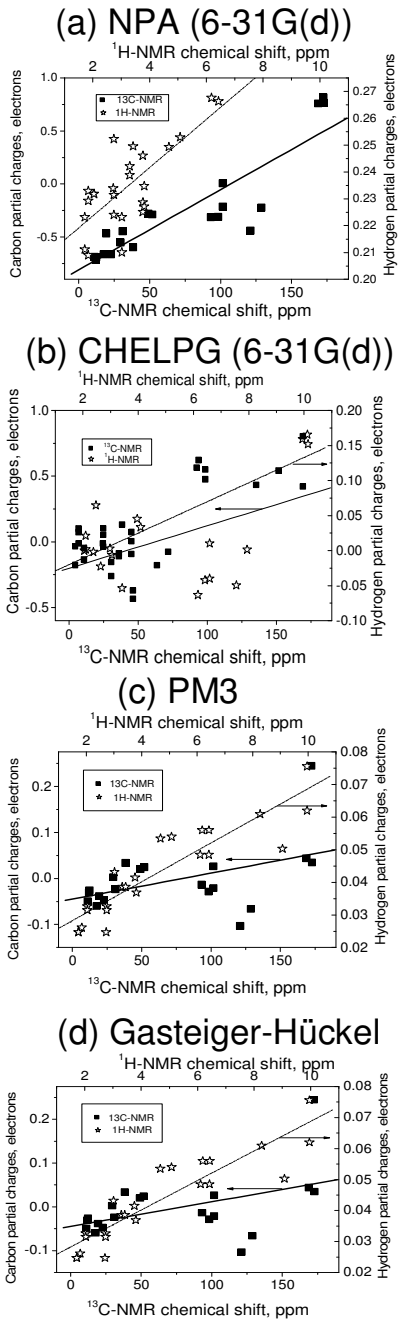

Fig. 5. Correlations between ^{13}C-NMR (asterisks, left axes) and ^{1}H-NMR (black squares, right axes) chemical shifts and partial charges calculated at DFT/B3LYP level of theory in combination with 6-31G(d) basis set and using NPA (a) and CHELPG (b) methods; by PM6 (c) and Gasteiger-Hückel (d) approaches.

Application of topological Gasteiger-Hückel approach gave very small and slightly positive partial charges of hydrogen atoms, their values being poorly dependent on their location in the molecule. Charges of some of carbon, oxygen

and nitrogen atoms were higher, but also substantially lower than those calculated by quantum-mechanical methods (Fig. 4, Table of partial charges in Electronic Supplementary Information (ESI)). Partial charges estimated by this approach poorly correlated with ^{13}C-NMR data and much better correlated with ^{1}H-NMR chemical shifts.

Comparison of charge distribution calculated in the absence and in the presence of water for DFT-based and semi-empirical methods had only marginal effect on the values of partial charges, indicating that hydration only slightly influences electron density distribution in Ce6.

So, the comparison made in the present work revealed that application of combination Natural population analysis and DFT/B3LYP/6-31G(d) level of theory gives partial charges in Ce6 molecule which correlate satisfactorily with NMR data. This result is in good agreement with the recently published comparison of different methods of calculation of partial atomic charges in ionic liquids. Charge distribution in these highly polarizable molecules was best calculated with Natural population analysis scheme at DFT/B3LYP level in combination with 6-31G(d) basis set, while MPA and CHELPG schemes were less accurate for the same level and basis set. [66] Application of combination of grid-based CHELPG with DFT/B3LYP/6-31G(d) level of theory and topological Gasteiger-Hückel approach give charges of carbon atoms in Ce6 which poorly correlate with NMR data, while they can be useful for estimation of charges on hydrogen atoms. On the contrary, ab initio Mulliken population analysis and semi-empirical PM3 and PM6 approaches give charges of hydrogen atoms which poorly correlate with NMR data, while they are useful for estimation of charges on carbon atoms. Taking into account that multi-electron atoms, such as carbon, oxygen or nitrogen, contribute to the orbitals of the whole molecule more significantly than hydrogen atoms, the methods giving more reliable data concerning carbon partial charges, i.e. NPA and MPA at DFT/B3LYP level in combination with 6-31G(d) basis set and PM6, were considered in the present study to be more trustworthy. Further we used the obtained data on charge distribution in Ce6 molecule for investigation of its interactions with polymer coils.

3. Docking of Ce6 on polymeric targets

Analysis of docking results revealed a large number of possible Ce6 binding sites closely approximated by their energy. Fig. 6 displays localization of the best configurations from 3 best clusters of Ce6-Pluronic (Fig. 6a) and Ce6-PVP (Fig. 6b) complexes obtained by AUTODOCK 4.2. Variously colored Ce6 stick models in this figure correspond to the configurations obtained from different schemes of partial charge evaluation. It is seen that in spite of striking difference in the absolute values of charges (Fig. 4), docking of these Ce6 models resulted in quite close Ce6 localization, implying that Coulomb forces made only moderate contribution to the energy of Ce6 interactions with Pluronic and PVP. This result seems to be quite reliable taking into account large diversity of schemes of partial charge evaluation used in the present work.

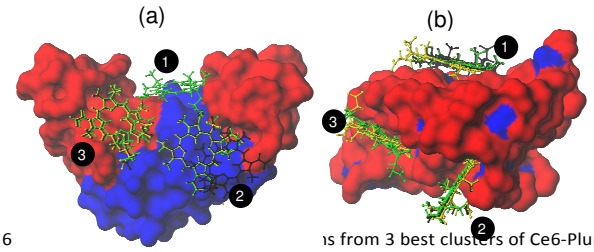

Fig. 6 ıs from 3 best clusters of Ce6-Pluronic (a) and Ce6-PVP (b) complexes obtained by AUTODOCK 4.2. The configurations obtained by NPA, MPA at DFT/B3LYP level of theory in combination with 6-31G(d) basis set, and by PM6 methods are shown as red, blue and green ball-and-stick models respectively.

All Ce6 models lie flatwise on the polymer coils. This configuration presumably ensures close contact between the polymer and porphyrin ring. (Fig. 6). Binding sites on PVP homopolymer do not exhibit any pronounced preference (Fig. 6b), while binding sites on Pluronic coil are mainly located at the interface between hydrophobic and hydrophilic blocks (Fig. 6a). Such position of Ce6 is in good agreement with our previous suggestions made on the basis of NMR results [22] and more previously from fluorescence measurements [67]. Obviously, Ce6 interaction with PPO block is stabilized by hydrophobic forces, while PEO blocks bind Ce6 through dipolar interactions and in certain cases via hydrogen bonds between ether oxygens and protonated carboxylic groups of Ce6. Polyethylene oxide blocks are flexible and therefore can freely adjust their conformation to form oriented H-bonds with Ce6 carboxylic groups. The same interactions with PPO blocks are sterically hindered by methyl groups of propylene oxide repeat units. So, these atoms hardly can be involved in the formation of H-bonds with Ce6, suggesting that Van-der-Walls forces mainly determine Ce6 interactions with these blocks.

Indeed, estimation of contribution of different forces to free energy of Ce6 binding made by Autodock 4.2 evaluation function shows dominant role of van-der-Waals interactions and hydrogen bonds, while electrostatics is of marginal importance. This explains why the method of partial charges evaluation in Ce6 insignificantly influences its localization on the surface of the studied polymers. However, despite negligible contribution of Coulomb forces, free binding energy depended on the approach of partial charge evaluation due to the contribution of cumulative term which includes Van der Waals forces, desolvation and H-bonding energy (Table 2).

Comparison of the energies of Ce6 binding to PVP and Pluronic F127 in the most efficient binding sites shows that PVP forms considerably more stable complexes than Pluronic F127 as assessed by AUTODOCK 4.2 (Table 3). Higher affinity of PVP to Ce6 has been recently shown in the direct experiments, where dissociation constants of Ce6 complexes with both polymers were estimated from the changes in its electronic spectra. [22] However, the absolute values of binding energies calculated by Autodock 4.2 evaluation function were nearly 5-fold underestimated in comparison to those observed in the experiment (Table 4). These discrepancies are probably

due to underestimation of desolvation energy term that should strongly contribute into the Ce6 interaction with the polymers. It could be supposed that AUTODOCK algorithm, which scores the solvation free energy per unit of volume, gives unrealistic scoring of its contribution into binding energy due to insufficiently correct estimation of desolvation term due to misappropriation of either scheme of calculation of occupied atomic volumes or atomic solvation parameters to the coils of synthetic polymers.

TABLE 2. Free energy of Ce6 binding to Pluronic F127 and PVP, and its electrostatic, Van-der-Waals, H-bonding, desolvation, torsion contributions in kcal/mol assessed by AUTODOCK 4.2 scoring functions.

Polymer	Method of calculation of partial atomic charges	$\Delta G_{binding}$	$\Delta G_{vdW} + \Delta G_{hbond} + \Delta G_{desolv}$	ΔG_{elec}	ΔG_{tors}
PVP	NPA[a]	-4,45	-7,13	0	2,68
	MPA[a]	-3,56	-5,6	-0,65	2,68
	CHELPG[a]	-4,49	-7,29	0,12	2,68
	PM6	-4,4	-7,1	0,01	2,68
	PM3	-5,47	-8,22	0,07	2,68
	Gasteiger-Hückel	-6,08	-8,08	-0,68	2,68
Pluronic F127	NPA[a]	-2,83	-5,38	-0,14	2,68
	MPA[a]	-4,32	-6,84	-0,16	2,68
	CHELPG[a]	-3,55	-6,01	-0,22	2,68
	PM6	-3,33	-5,97	-0,04	2,68
	PM3	-4,6	-7,11	-0,17	2,68
	Gasteiger-Hückel	-5,57	-8,13	-0,12	2,68

[a] Electron wave functions were calculated at DFT/B3LYP level in combination with 6-31G(d) basis set.

In contrast to AUTODOCK, empirical functions do not require evaluation of occupied atomic volumes and solvation parameters for the scoring of hydrophobic interactions. Therefore we calculated the free energy of Ce6-polymer interactions using one of the most commonly used scoring functions, Chem-Score, a regression-based scoring function, which evaluates the strength of the ligand–receptor interaction by using contact terms for lipophilic, metal-binding and hydrogen-bonding contributions, and includes also an entropic term which gives estimate of the loss of ligand's conformational flexibility upon binding. Hydrophobic interactions are calculated in this algorithm as a value of contact area multiplied by the empirical parameter determined from regression analysis. This parameter was evaluated from correlation analysis of 82 ligand–receptor complexes with known binding affinities and was tested using two other sets of 20 and 10 protein–ligand complexes, respectively. [52]

TABLE 3. Free energy of Ce6 binding with PVP and Pluronic obtained experimentally and predicted for the most efficient configuration by various molecular mechanics approaches.

Polymer	Experimental value, kcal/mol [33]	Method of partial charges evaluation	Autodock4.2 calculated binding energy, kcal/mol	Sybyl 8.1 Chem-score calculated binding energy, kcal/mol
PVP	-32.9	NPA[a]	-4,45	-33.66
		MPA[a]	-3,56	-33.27
		PM6	-4.4	-34.57
Pluronic F127	-27.9	NPA[a]	-2.83	-25.96
		MPA[a]	-4.32	-26.58
		PM6	-3,33	-28.45

[a] Electron wave functions were calculated at DFT/B3LYP level in combination with 6-31G(d) basis set.

Evaluation of binding energy made by Chem-Score function gave the values quite similar to those observed in the experiment (Table 4). The best results were obtained for the configurations predicted by AUTODOCK 4.2 with Ce6 partial charges evaluated with NPA and MPA methods at DFT/B3LYP level in combination with 6-31G(d) basis set, but not according to Gasteiger-Hückel (Table 4). So, the obtained results strongly suggest that ab initio quantum mechanical approaches to partial charges evaluation and docking procedure using AUTODOCK 4.2 allows locating of binding sites on polymeric coils, whereas application of empirical Chem-Score function gives quite realistic estimate of the free energy of Ce6 binding to the polymers. The latter conclusion agrees with the ranking of scoring functions made in. [68]

The results of molecular modeling give excellent agreement with the experimental data obtained previously [22] and showed that Ce6 binds tightly to the coils of both polymers, Ce6 binding with PVP being appreciably more effective than that with Pluronic. According to molecular dynamics simulations, Ce6 lies flatwise on the surfaces of coils of both polymers. Obviously, such localization ensures close contact of Ce6 with the polymers and formation of multi-point Van-der-Waals and hydrogen interactions. Importantly, molecular mechanics calculations support indirect experimental evidence of Ce6 ability to interact not only with PPO but also with PEO blocks in Pluronic molecules. This observation is in agreement with the previously reported attraction between hematoporphyrin and PEG obtained by MD simulations. [39]

CONCLUSIONS

In the present paper we applied molecular dynamics and docking algorithms to study interactions between chlorin e6 with two synthetic polymers - polyvinylpyrrolidone and Pluronic F127. The work was motivated by recently demonstrated ability of these polymers to enhance photocatalytic activity of chlorin e6 in cell cultures. **Error!**

Bookmark not defined. In this paper, we found that only hydrophilic Pluronics and completely hydrophilic homopolymer PVP enhance phototoxicity of Chlorin e6. Unexpectedly, hydrophobic Pluronics were unable to produce this effect. So, we hypothesized that polar interactions strongly contribute to this interaction. However, molecular modeling showed that mainly Van-der Waals forces, and mostly hydrophobic interaction are responsible for Ce6 interactions with hydrophilic polymers. In these complexes, Chlorine locates in the interface between hydrophobic and hydrophilic parts. It was amazing that even in the complexes with PVP Chlorin finds islets formed by the groups of the main backbone and settles over them. Our further studies of this system (paper in preparation) show that these complexes remain within 1-2 h in the presence of bovine serum, but further release Ce6. Uptake of Chlorin-polymer complexes by tumor cells results in its quick transfer .to biological membranes. Therefore, when the cells are laser illuminated, singlet oxygen is generated inside the membranes, so the latter undergo disruption, that it turns leads to cell death. The results obtained in the present paper can explain why this transfer is so effective: cell membranes are the better acceptors of Chlorin e6 in comparison to hydrophilic polymers.

Molecular dynamics simulations of PVP and Pluronic chains revealed hierarchy of coiling of stereoregular and isotactic models of both polymers. The obtained results suggest that chain fragments with regular arrangement of pendant groups should form helical conformation due to restriction of rotation around the substituted C-C bonds of the polymer backbone, one of the possible sources of this restriction being Van-der-Waals repulsion of the substituents. In the present report, we showed that helical motifs aggregate to produce hairpin-like structures with the minimal water-accessible hydrophobic surface area, which further assemble in the coil.

In general, the revealed helix formation in the stereoregular carbon-chain PVP and hetero-chain polypropylene oxide seems to be a common phenomenon for polymers containing regular fragments with restricted rotation around the backbone bonds. This restriction may be accounted for either by steric factors (the presence of regularly arranged pendant groups that hamper rotation around the backbone bonds) or may be associated with the presence of multiple bonds or cycles in the polymer backbone. [69] Formation of helical structures also may be associated with formation of aligned non-covalent bonds between the backbone and low molecular ligands as was observed in studies of PEG interaction with sodium ions that were capable of coordinating by ether oxygens.[28]

Comparison of a number of methods of evaluation of partial charges in Chlorin e6 molecule through analysis of linear correlations between partial charges and experimentally available ^{1}H- and ^{13}C-NMR chemical shifts showed that CHELPG at DFT/B3LYP level of theory in combination with 6-31G(d) basis set

PM3 and Gasteiger-Hückel approaches are powerful in the evaluation of hydrogen charges, while their ability to estimate charges on carbon atoms in Ce6 is poor. On the contrary, Mulliken population analysis DFT/B3LYP level in combination with 6-31G(d) basis set and PM6 methods allow evaluating charges of carbon atoms quite correctly, but give poor estimate of charges on hydrogen atoms. Only Natural population analysis at DFT/B3LYP level of theory allows estimating of charges on hydrogen and carbon atoms with similar accuracy. However, it gives better results when 6-31G(d) rather than 6-311G(2d,2p) basis set is applied. This result is consistent with a number of previous studies, where high sensitivity of results obtained with MPA and NPA methods to the type of basis set has been demonstrated. [70]

Analysis of Chlorin e6 docking on polymer coils revealed that polymer complexes are stabilized by an ensemble of multi-point Van-der-Waals interactions, chlorin e6 ring being allocated flatwise on the surface of polymer molecules. In the complexes with Pluronic F127, it lies on the interface between hydrophobic and hydrophilic regions of the molecule that is consistent with the previously published NMR-spectroscopy results [22]. Theoretical estimation of the free energy of Chlorin e6 binding to Pluronic and PVP showed its higher affinity to PVP also in agreement with experimental data[22]. Calculations revealed marginal contribution of Coulomb forces in the stabilization of both complexes, major role being played by van-der-Waals and hydrogen interactions.

The results demonstrated the ability of Autodock 4.2 to predict localization of binding sites of Ce6 on polymeric coils. However, Autodock scoring functions gave energies of binding that did not match experimental results. In contrast, application of Chem-Score scoring function gave free energies of Ce6 binding to PVP and Pluronic quite close to those observed in the experiment.

Acknowledgements

This work was partially supported by the Russian Foundation for Basic Research (Projects Nos. 13-03-00429-a, 11-02-01090-a and 11-03-12074-ofi-m).

Notes and references

[a] Institute for Physical-Chemical Medicine, Malaya Pirogovskaya Str., 1a, Moscow 119435, Russia.

[b] A.V. Topchiev Institute of Petrochemical Synthesis, RAS, Leninsky Prosp. 29, 119991 Moscow, Russia.

[c] N.N. Semenov Institute of Chemical Physics RAS, Kosygina St.1, Moscow, 119991 Russia.

[d] Chemistry Department, M.V. Lomonosov Moscow State University, Vorobiovy Gory,

[*]Correspondence to: Melik-Nubarov N.S. (E-mail: melik.nubarov@genebee.msu.ru) and Tsvetkov V.B. (E-mailL: v.b.tsvetkov@gmail.com)

Electronic Supplementary Information (ESI) available: (Supplementary materials: Table 1S. Partial atomic charges in Chlorin e6 calculated by different methods). [details of any supplementary information available should be included here]. See DOI: 10.1039/b000000x/

References

(1) T.J. Dougherty, *Crit. Rev. Oncol. Hematol.,* 1984, **2**, 83.
(2) J.J. Reiners Jr., P. Agostinis, K. Berg, N.L. Oleinick, D. Kessel, *Autophagy*, 2010, **6**, 7.
(3) C.L. Silva, J.O. Del Ciampo, F.C. Rossetti, M.V. Bentley, M.B. Pierre, *Photochem. Photobiol.* 2013, **89**, 1176.
(4) S.M. El-Daly, A.M. Gamal-Eldeen, M.A. Abo-Zeid, I.H. Borai, H.A. Wafay, A.R. Abdel-Ghaffar, *Photodiagnosis Photodyn. Ther.* 2013, **10**, 173.
(5) I.H. Oh, H.S. Min, L. Li, T.H. Tran, Y.K. Lee, I.C. Kwon, K. Choi, K. Kim, K.M. Huh, Biomaterials, 2013, **34**, 6454.
(6) F. Li, B.C. Bae, K. Na, *Bioconjug. Chem*. 2010, **21,** 1312.
(7) B.C. Bae, K. Na, *Biomaterials*, 2010, **31**, 6325.
(8) F. Schmitt, L. Lagopoulos, P. Käuper, N. Rossi, N. Busso, J. Barge, G. Wagnières, C. Laue, C. Wandrey, L. Juillerat-Jeanneret, *J. Control. Release,* 2010, ***144,*** 242.
(9) S. Daoud-Mahammed, P. Couvreur, K. Bouchemal, M. Chéron, G. Lebas, C. Amiel, R. Gref, *Biomacromolecules,* 2009, **10,** 547.
(10) H.C. Tsai, C.H. Tsai, S.Y. Lin, C.R. Jhang, Y.S. Chiang, G.H. Hsiue, *Biomaterials,* 2012, **33,** 1827.
(11) H. Ding, B.D. Sumer, C.W. Kessinger, Y. Dong, G. Huang, D.A. Boothman, J. Gao, *J. Control. Release,* 2011, **151**, 271.
(12) B. Pegaz, E. Debefve, F. Borle, J.P. Ballini, H. van den Bergh, Y.N. Kouakou-Konan, *J. Photochem. Photobiol. B*, 2005, **80**, 19.
(13) M. Susan, I. Baldea, S. Senila, V. Macovei, S. Dreve, R.M. Ion, R. Cosgarea, *Int. J. Dermatol*. 2011, **50**, 280.
(14) J. Sobczyński, H.H. Tønnesen, S. Kristensen, *Pharmazie*, 2013, **68**, 100.
(15) Vargas, B. Pegaz, E. Debefve, Y. Konan-Kouakou, N. Lange, J.P. Ballini, H. van den Bergh, R. Gurny, F. Delie, *Int. J. Pharm.* 2004, **286**(1-2):131-45.
(16) R.K. Chowdhary, I. Sharif, N. Chansarkar, D. Dolphin, L. Ratkay, S. Delaney, H. Meadows, *J. Pharm. Pharm. Sci.* 2003, **6**, 198.
(17) M. Zeisser-Labouèbe, N. Lange, R. Gurny, F. Delie, *Int. J. Pharm*. 2006, **326**, 174.
(18) H.A. Isakau, M.V. Parkhats, V.N. Knyukshto, B.M. Dzhagarov, E.P. Petrov, P.T. Petrov, *J. Photochem. Photobiol. B,* 2008, **92**, 165.
(19) W.W.L. Chin, P.W.S. Heng, R. Bhuvaneswari, W.K.O. Lau, M. Olivo, *Photochem. Photobiol. Sci.* 2006, **5**, 1031.
(20) W.W.L. Chin, T. Praveen, P.W.S. Heng, M. Olivo *Eur. J. Pharm. Biopharm.* 2010, **76**, 245.
(21) W.W.L. Chin, P.W.S. Heng, M. Olivo, *BMC Pharmacology*, 2007, **7**, 15.
(22) T.M. Zhiyentayev, U.T. Boltaev, A.B. Solov'eva, N.A. Aksenova, N.N. Glagolev, A.V. Chernjak, N.S. Melik-Nubarov, *Photochem. Photobiol*. 2013, doi: 10.1111/php.12181.
(23) F. Avila-Salas, C. Sandoval, J. Caballero, S. Guiñez-Molinos, L.S. Santos, R.E. Cachau, and F.D. González-Nilo, *J. Phys. Chem. B*, 2012, **116**, 2031.
(24) V. Maingi, M.V.S. Kumar, P.K. Maiti, *J. Phys. Chem. B*, 2012, **116**, 4370.
(25) C. Martín, M. Gil, B. Cohen, A. Douhal, *Langmuir*, 2012, **28**, 6746.
(26) C. Li, J.-X. Wang, Y. Le, J.-F. Chen, *Mol. Pharmaceutics*, 2013, **10**, 2362.
(27) A.D. Costache, L. Sheihet, K. Zaveri, D.D. Knight, J. Kohn, *Mol. Pharm.* 2009, **6**, 1620.
(28) Y.-C. Li, S. Rissanen, M. Stepniewski, O. Cramariuc, T. Róg, S. Mirza, H. Xhaard, M. Wytrwal, M. Kepczynski, A. Bunker *J. Phys. Chem. B*, 2012, **116**, 7334.
(29) M. Macháčková, J. Tokarsky, P. Čapková, *J. Pharm. Sci.* 2013, **48**, 316.
(30) V. López-Mejías, J.L. Knight, C.L. Brooks, A.J. Matzger, *Langmuir*, 2011, **27**, 7575.
(31) J. Gasteiger, M. Marsili, *Tetrahedron Lett*. 1978, **19**, 3181.
(32) D.A. Case, T.A. Darden, T.E. Cheatham III, C.L. Simmerling, J. Wang, R.E. Duke, R. Luo, K.M. Merz, B. Wang, D.A. Pearlman, M. Crowley, S. Brozell, V. Tsui, H. Gohlke, J. Mongan, V. Hornak, G. Cui, P. Beroza, C. Schafmeister, J.W. Caldwell, W.S. Ross and P.A. Kollman, AMBER 8, University of California, San Francisco, 2004.
(33) G.D. Hawkins, C.J. Cramer and D.G. Truhlar, *J. Phys. Chem.* 1996, **100**, 19824.
(34) D. Bashford, D.A. Case, *Ann. Rev. Phys. Chem.* 2000, **51**, 129.
(35) J. Wang, R.M. Wolf, J.W. Caldwell, P.A. Kollman, D. Case, *J. Comput. Chem*. 2004, **25,** 1157.
(36) J.-P. Ryckaert, G. Ciccotti, H.J.C. Berendsen, *J. Comput. Phys.* 1977, **23**, 327.
(37) M.J.D. Powell, *Math. Program.* 1977, **12**, 241.
(38) M. Clark, R.D. Cramer, N. Van Opdenbosch, *J. Comput. Chem.* 1989, **10**, 982.
(39) J.J.P. Stewart, *Rev. Comput. Chem.* 1990, **1**, 45.
(40) J.J.P. Stewart, *J. Mol. Model.* 2007, **13**, 1173.
(41) C. Lee, W. Yang, R.G. Parr, *Phys. Rev. B*, 1988, **37**, 785.
(42) A.D. Becke, *J. Chem. Phys.* 1993, **93**, 5648.
(43) R.G. Parr, W. Yang, *Density-functional theory of atoms and molecules.* Oxford University Press, New York, 1989.
(44) R.S. Mulliken, *J. Chem. Phys.* 1955, **23**, 1833.
(45) A.E. Reed, F. Weinhold, *J. Chem. Phys.* 1983, **78**, 4066.
(46) A.E. Reed, R. B. Weinstock, F. Weinhold, *J. Chem. Phys.* 1985, **83**, 735.
(47) C.M. Breneman, K.B. Wiberg, *J. Comput. Chem.* 1990, **11**, 361.
(48) M.J. Frisch, G.W. Trucks, H.B. Schlegel, G.E. Scuseria, M.A. Robb, J.R. Cheeseman, G. Scalmani, V. Barone, B. Mennucci, G. A. Petersson, H. Nakatsuji, M. Caricato, X. Li, H. P. Hratchian, A. F. Izmaylov, J. Bloino, G. Zheng, J. L. Sonnenberg, M. Hada, M. Ehara, K. Toyota, R. Fukuda, J. Hasegawa, M. Ishida, T. Nakajima, Y. Honda, O. Kitao, H. Nakai, T. Vreven, J. A. Montgomery, Jr., J. E. Peralta, F. Ogliaro, M. Bearpark, J. J. Heyd, E. Brothers, K. N. Kudin, V. N. Staroverov, R. Kobayashi, J. Normand, K. Raghavachari, A. Rendell, J. C. Burant, S. S. Iyengar, J. Tomasi, M. Cossi, N. Rega, J. M. Millam, M. Klene, J. E. Knox, J. B. Cross, V. Bakken, C. Adamo, J. Jaramillo, R. Gomperts, R. E. Stratmann, O. Yazyev, A. J. Austin, R. Cammi, C. Pomelli, J. W. Ochterski, R. L. Martin, K. Morokuma, V. G. Zakrzewski, G. A. Voth, P. Salvador, J. J. Dannenberg, S. Dapprich, A. D. Daniels, Ö. Farkas, J. B. Foresman, J. V. Ortiz, J. Cioslowski, and D. J. Fox *Gaussian 09*, Revision A.1, Gaussian, Inc., Wallingford CT, 2009.

(49) G.M. Morris, R. Huey; W. Lindstrom, M.F. Sanner, R.K. Belew, D.S. Goodsell, A.J. Olson, *J. Comput. Chem.* 2009, **30**, 2785.
(50) P. F. W. Stouten, C. Froemmel, H. Nakamura, C. Sander, *Mol. Simul.,* 1993*,* **10,** 97.
(51) T.A. El-Mihoub, A.A. Hopgood, L. Nolle, A. Battersby, *Engineering Letters*, 2006, **13**, 124.
(52) M.D. Eldridge, C.W. Murray, T.R. Auton, G.V. Paolini, R.P. Mee, *J. Comput.-Aided Mol. Des.*, 1997, **11**, 425.
(53) B.-C. Lee, R.N. Zuckermann, K.A. Dill, *J. Am. Chem. Soc.* 2005, **127**, 10999.
(54) A.-A. A. Abdel Azim, H. Tenhu, J. Maerta, F. Sundholm, *Polymer Bull*. 1992, **29**, 461.
(55) P.G. De Gennes, *Scaling Concepts in Polymer Physics*, CORNELL UNIVERSITY PRESS, Ithaca and London, 1979.
(56) V. Vitagliano, L. Costantino, R. Sartorio, *J. Phys. Chem.* 1976, **80**, 959.
(57) G. Natta, *Makromol. Chem.* 1960, **35**, 94.
(58) J. Gasteiger, M. Marsili, *Org. Mag. Resonance.* 1981, **15**, 353-360.
(59) D. Sitkoff, D.A. Case, *J. Am. Chem. Soc.* 1997, 19, 12262.
(60) R.J. Abraham, P.M. Edgar, R.P. Glover, M.A. Warne, L. Griffiths, *J. Chem. Soc., Perkin Trans.* 1995, **2**, 333.
(61) E.S.E. Eriksson, L.A. Eriksson, *Phys. Chem. Chem. Phys.* 2011, **13**, 7207.
(62) V. Barone, M. Cossi, *J. Phys. Chem. A,* 1998, **102,** 1995-2001.
(63) M. Cossi, N. Rega, G. Scalmani, V. Barone, *J. Comp. Chem.,* 2003, **24**, 669.
(64) H.A. Isakau, T.V. Trukhacheva, P.T. Petrov, *J. Pharm. Biomed. Anal.* 2007, **45**, 20.
(65) K.M. Smith, J.F. Unsworth, *Tetrahedron*, 1975, **31**, 367- 375.
(66) J. Rigby, E.I. Izgorodina, *Phys.Chem. Chem. Phys.* 2013, **15**, 1632.
(67) T.M. Zhiyentaev, N. S. Melik-Nubarov, E.A. Litmanovich, N.A. Aksenova, N.N. Glagolev, A.B. Solov'eva, *Polymer Science (Rus.), Ser. A*, 2009, **51**, 502.
(68) S.Y. Huang, S.Z. Grinter, X. Zou, *Phys. Chem. Chem. Phys.* 2010, **12**, 12899.
(69) P. Linse, P. Palenčá, T. Bleha *J. Phys. Chem. B,* 2011, **115**, 11448.
(70) R.B. Viana, E.D.A. Santos, L.J. Valencia, R.M. Cavalcante, E.B. Costa, R. Moreno-Fuquen, A.B.F. da Silva, *Spectrochim. Acta A,* 2013, **102**, 386.